

Water Impact of Rigid Wedges in Two-Dimensional Fluid Flow

S. A. Shah, A. C. Orifici[†] and J. H. Watmuff

RMIT University, School of Aerospace, Mechanical and Manufacturing Engineering, GPO Box 2476, Melbourne, Victoria 3001, Australia

[†]*Corresponding Author Email: adrian.orifici@rmit.edu.au*

(Received January 15, 2014; accepted March 16, 2014)

ABSTRACT

A combined experimental and numerical investigation was conducted into impact of rigid wedges on water in two-dimensional fluid conditions. Drop test experiments were conducted involving symmetric rigid wedges of varying angle and mass impacted onto water. The kinematic behaviour of the wedge and water was characterised using high-speed video. Numerical models were analysed in LS-DYNA[®] that combined regions of Smoothed Particle Hydrodynamics particles and a Lagrangian element mesh. The analysis captured the majority of experimental results and trends, within the bounds of experimental variance. Further, the combined modelling technique presented a highly attractive combination of computational efficiency and accuracy, making it a suitable candidate for aircraft ditching investigations.

Keywords Water impact, Drop tests, Smoothed particle hydrodynamics.

NOMENCLATURE

| | | | |
|----------------|--|-----------|-------------------------------|
| a | impactor acceleration during impact | h | model trough height |
| a_f | impactor free-fall acceleration | h_{SPH} | model SPH section height |
| $F_{friction}$ | impactor guiding system friction force | M | impact mass |
| F_{impact} | impact force | w | model width |
| g | gravitational constant | w_{SPH} | model SPH section width |
| | | θ | impactor wedge deadrise angle |

1. INTRODUCTION

Aircraft crash landing on water, or aircraft “ditching”, is a complex impact scenario involving interaction between water and a deformable structure. Large scale testing of aircraft water impact is expensive and involves challenging test procedures and data measurement (Pentecôte and Vigliotti 2003; Anghileri et al. 2011). As such, the application of advanced numerical simulation is a critical step in ditching investigations. As with any investigation, the capabilities of any analysis tool must be rigorously validated to ensure its capabilities for capturing all relevant phenomena.

Smoothed particle hydrodynamics (SPH) is a mesh-free Lagrangian computational method that has been used for simulating fluid flows (Gingold and Monaghan 1977). In this approach, the fluid is discretised into particles, properties of the particle are defined over a spatial distance, and the interaction of the particles is defined using equations of state. The particle-based

nature of the definition is advantageous for capturing large deformations as it avoids problems such as mesh distortion associated with Lagrangian mesh-based methods. It also is advantageous compared to Eulerian fixed-mesh methods, as only the material domain is required to be meshed (Liu and Liu 2003). A comprehensive review of SPH is presented by Liu and Liu (2010), which includes detailed descriptions, comparison with other fluid modelling approaches and almost 400 references.

Several authors have applied SPH models to numerically investigate large scale ditching scenarios (Anghileri et al. 2011; Fasanella et al. 2003; Pentecôte et al. 2003; Anghileri et al. 2014). This type of investigation typically involves complex three-dimensional (3D) fluid flows and pressure distributions, deformable structures with fluid-structure interaction (FSI) phenomena, and validation against challenging experimental output. However, there is limited published data validating the capabilities of SPH modelling technology for water impact at a more

fundamental level, in particular for two-dimensional (2D) fluid flows and rigid structures.

Oger *et al.* (2006) demonstrated SPH analysis of rigid wedges in 2D fluid flows. However, the work only considered two different wedge angles, and used results from different experimental setups. Further, the numerical analysis used 21 million SPH particles, which would not be a suitable modelling approach for aircraft ditching investigations. Panciroli (2013) summarised results of several SPH studies, and commented that verification of the results is not yet at the level of standard computational fluid dynamics. The combination of SPH regions with traditional Lagrangian mesh-based regions offers the potential for a computational modelling strategy suitable for large structures. Several authors have used this approach to combine an SPH region for the fluid with a finite element region for the structure (Groenenboom and Cartwright 2010; Campbell and Vignjevic 2012). However, there have only been limited publications on the use of different regions to capture the fluid in a computationally efficient manner, particularly in comparison with experimental results capable of providing rigorous assessment of the accuracy of this approach. As such, there is a need to investigate a combined SPH and mesh-based modelling strategy for water impact problems, and to validate this across a broad range of experimental test cases within the same experimental setup.

In this paper, results from an experimental and numerical investigation into water impact of rigid wedges are presented. A goal of the study was to develop experimental data for validation of numerical analysis tools for water impact across a broad range of wedge angles. A second goal was to investigate a numerical modelling strategy that was more computationally efficient for larger structures. Drop test experiments were conducted involving symmetric rigid wedges of varying angle and mass impacted into a trough of water, to generate a 2D flow field. The kinematic behaviour of the wedge and water was recorded and characterised using a high-speed video camera. Numerical analysis was conducted in LS-DYNA® using models that combined SPH and meshed regions. The numerical predictions are compared to the experimental results to assess the capabilities of the modelling strategy.

2. EXPERIMENTAL TESTING

The test rig and specimens are summarised in Fig. 1 and Table 1. Symmetric wedge impactors of varying angles were dropped vertically into a water tank. The length of the wedges was sized to give only a 2 mm gap on each side of the water tank, to promote a 2D fluid field upon impact. The angle θ , or “deadrise” angle, was defined between the horizontal and the wedge inclined face, as shown in Fig. 1. Five deadrise angles were investigated. The wedges were manufactured from pinewood, sanded for consistency, and varnished to prevent water absorption. Sheet metal plates were added so that each wedge had the same mass. Additional weights were added to the wedges in different test configurations, so that three different wedge masses were investigated. The lightest (1.64 kg) wedge was dropped from heights of 50 mm, 100 mm and 150 mm, and the wedges with increased mass were

dropped from heights of 50 mm and 100 mm. A tank water height of 210 mm was used for all tests. Three tests were conducted for each test configuration, and all configurations are summarised in Table 1.

The impact event was filmed using a high-speed video camera at 500 frames/second, and used to characterise the kinematic behaviour of the impactor and fluid flow. The camera used was the X-Stream™ XS-4 model manufactured by Integrated Design Tools. Dots were drawn on the face of the wedge, and the Open Source software Tracker (Brown 2011) was used to track the movement of these dots and generate the displacement-time history of the wedge. To use this software, a reference distance in the image is defined, and the user manually identifies the dot centroid location to be tracked in each image. A sample image of the point tracking is shown in Fig. 2.

A 5-point central difference scheme was used to calculate the acceleration history from the displacement-time data. However, it was found that this method had high sensitivity to variation in displacement measured from the dot tracking method. Following this, a 5th order polynomial was fit to the displacement data, and used to determine expressions for velocity and acceleration. The polynomial was fit to displacement data in only the “impact region”, or region of rapidly increasing and decreasing acceleration. Data points were taken every two frames (time increment 0.004 s), which was found in preliminary studies to produce almost identical results compared to taking data at every single frame.

The vertical motion of the wedges was controlled by a guiding system of drawer slides aligned vertically. This system was found to have an appreciable amount of friction. This friction was quantified by studying the free-fall motion of the three wedges. From a drop test of each wedge with no water impact, the free-fall acceleration of the wedge was measured. The free-fall acceleration was used to determine the friction force for each mass using the equation of motion

$$F_{friction} - Mg = Ma_f \quad (1)$$

where $F_{friction}$ is the friction force, M is the wedge mass, g is acceleration due to gravity and a_f is the free-fall acceleration. The results for free-fall acceleration and friction force for each wedge are shown in Table 1, which also shows the measured impact velocity for each test condition.

For each drop test, the impact force on the wedge was determined using the equation of motion

$$F_{impact} + F_{friction} - Mg = Ma \quad (2)$$

where F_{impact} is the force on the impactor, a is the impactor acceleration measured at any data point, and the vertical forces due to buoyancy and skin friction on the wedge wetted area are assumed negligible. The impact force was converted to a “section force” (in N/mm) by normalising using the wedge depth of 333 mm, to determine the cross-section impact force.

3. NUMERICAL MODELLING

Numerical models were analysed in LS-DYNA® 971 (Hallquist 2006) for all test configurations in Table 1. A

Table 1 Test Configurations

| Wedge mass, kg | Drop height, mm | Deadrise angles θ , ° | Free-fall acceleration, m/s ² | Friction force, N | Impact velocity, m/s |
|----------------|-----------------|------------------------------|--|-------------------|----------------------|
| 1.6394 | 50 | 20, 25, 30, 35, 40 | 5.474 | 7.108 | 0.740 |
| 1.6394 | 100 | 20, 25, 30, 35, 40 | 5.474 | 7.108 | 1.046 |
| 1.6394 | 150 | 20, 25, 30, 35, 40 | 5.474 | 7.108 | 1.281 |
| 1.8519 | 50 | 20, 25, 30, 35, 40 | 5.757 | 7.506 | 0.757 |
| 1.8519 | 100 | 20, 25, 30, 35, 40 | 5.757 | 7.506 | 1.073 |
| 2.0722 | 50 | 20, 25, 30, 35, 40 | 6.230 | 7.418 | 0.789 |
| 2.0722 | 100 | 20, 25, 30, 35, 40 | 6.230 | 7.418 | 1.116 |

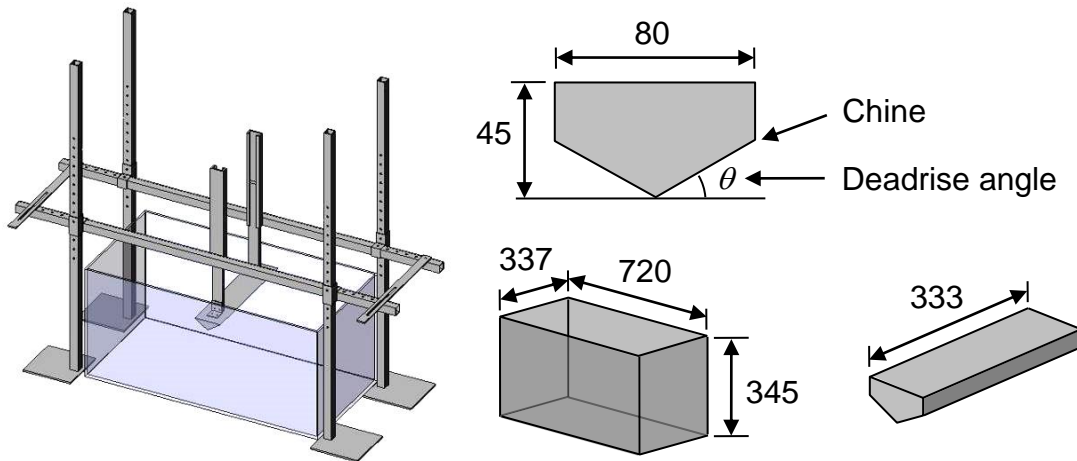


Fig. 1. Test rig and wedge specimen dimensions (mm).

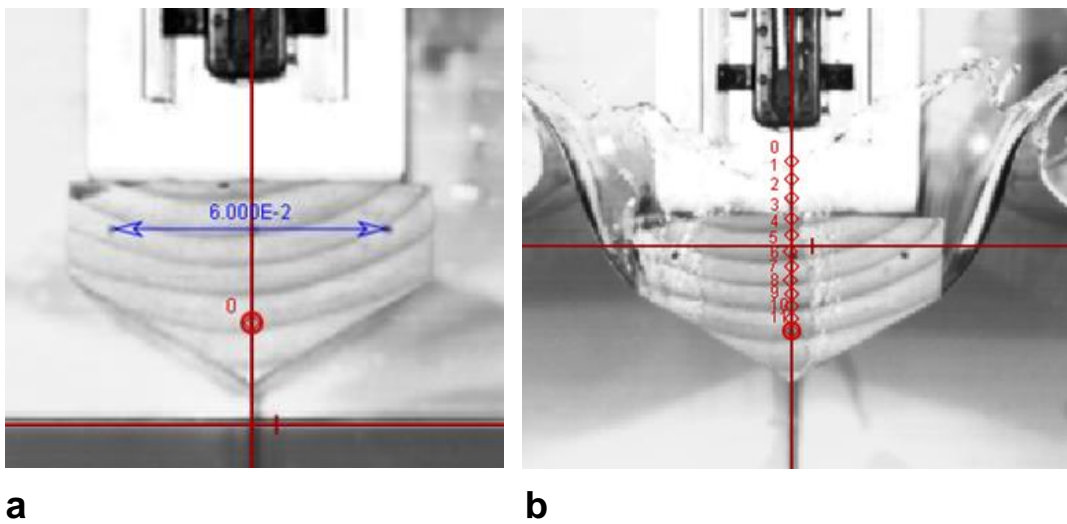


Fig. 2. Wedge face point tracking in Tracker. (a) Initial reference definition. (b) Point identification.

schematic of the numerical models is shown in Fig. 3. Models with a wedge depth (out of plane) of 3 mm were analysed to generate a 2D flow field, and the wedge section force was determined by normalising the wedge force by the depth. Vertical symmetry was exploited to model half of the wedge and water tank, though full-width models were investigated in preliminary studies and shown to give almost identical results. The wedge was modelled as a rigid body, with

the density determined to match the experimental inertial characteristics of each wedge. The water was modelled using a null material card with a Gruneisen equation of state to define the pressures within the fluid domain. The parameters of the water equation of state are given in Table 2. Gravity was applied on the wedge only, and not on the water particles, which was found in preliminary investigations to improve computational efficiency with only minimal effect on solutions.

Table 2 Numerical water model parameters

| | |
|--|----------|
| Density ρ , kg/m ³ | 998 |
| Dynamic viscosity coefficient μ , Pa s | 0.001002 |
| Speed of sound in water C , m/s | 1484 |
| Slope coefficient S_1 | 1.979 |
| Slope coefficient S_2 | 0 |
| Slope coefficient S_3 | 0 |
| Gruneisen gamma γ_0 | 0.11 |
| Volume correction coefficient a | 0 |
| Internal energy per initial volume E , J | 0 |

Table 3 Particle density investigation parameters

| Distance between particles, mm | Particle mass, kg | Initial smoothing length, mm | Solution time step, s | Computational time, hours |
|--------------------------------|------------------------|------------------------------|-----------------------|---------------------------|
| 4 | 6.388×10^{-5} | 4.8 | 4.39×10^{-6} | 0.37 |
| 2 | 7.986×10^{-6} | 2.4 | 2.19×10^{-6} | 1.57 |
| 1 | 9.982×10^{-6} | 1.2 | 1.10×10^{-6} | 23 |

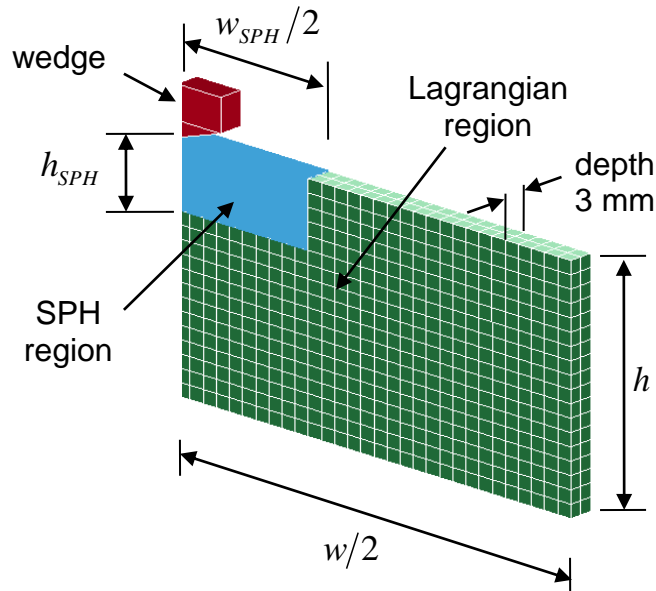


Fig. 3. Numerical model definition.

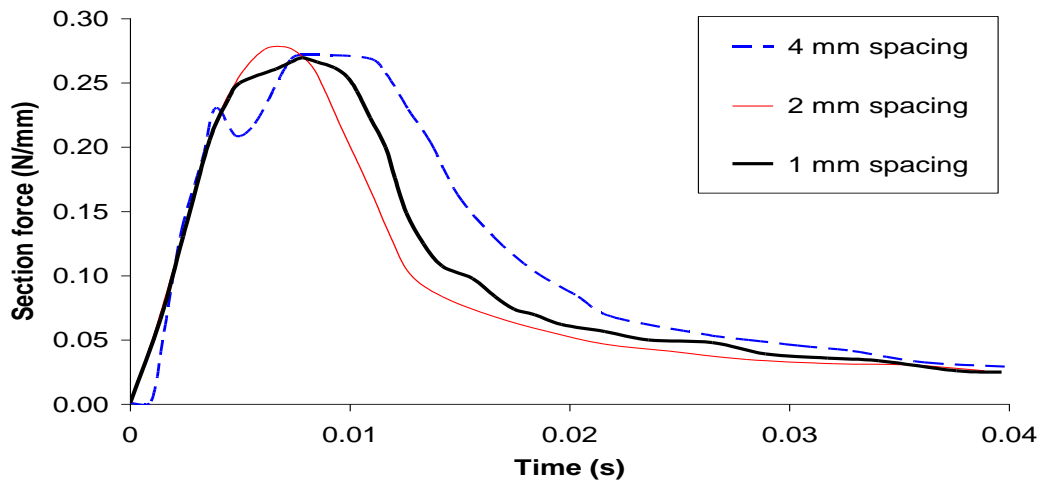


Fig. 4. Particle density investigation, section force, 1.64 kg impactor, 20° deadrise angle, 150 mm drop height.

Table 3 Particle density investigation parameters

| Distance between particles, mm | Particle mass, kg | Initial smoothing length, mm | Solution time step, s | Computational time, hours |
|--------------------------------|------------------------|------------------------------|-----------------------|---------------------------|
| 4 | 6.388×10^{-5} | 4.8 | 4.39×10^{-6} | 0.37 |
| 2 | 7.986×10^{-6} | 2.4 | 2.19×10^{-6} | 1.57 |
| 1 | 9.982×10^{-6} | 1.2 | 1.10×10^{-6} | 23 |

Table 4 Numerical model parameters

| | |
|--|----------------------------|
| Initial distance between SPH particles | 1 mm |
| Contact thickness between SPH and Lagrangian regions | 0.5 mm |
| Total trough height, h | 216 mm |
| Total trough half-width, $w/2$ | 360 mm |
| SPH section height, h_{SPH} | 60 mm |
| SPH section half-width $w_{SPH} / 2$ | 120 mm |
| Number of SPH particles | 21600 |
| Individual particle mass | 9.98×10^{-7} kg |
| Lagrangian element type | Fully integrated S/R solid |
| Number of solid Lagrangian elements | 490 |
| Contact type between wedge and water | Soft penalty-based |
| Smoothing length constant (CSLH) | 1.2 (default) |
| Minimum smoothing length (HMIN) | $0.2h_0$ (default) |
| Maximum smoothing length (HMAX) | $2h_0$ (default) |

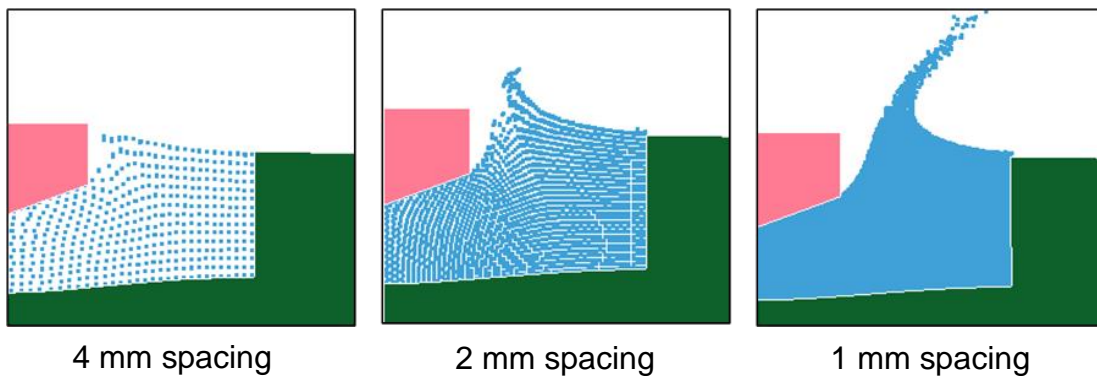


Fig. 5. Particle density investigation, fluid flow results.

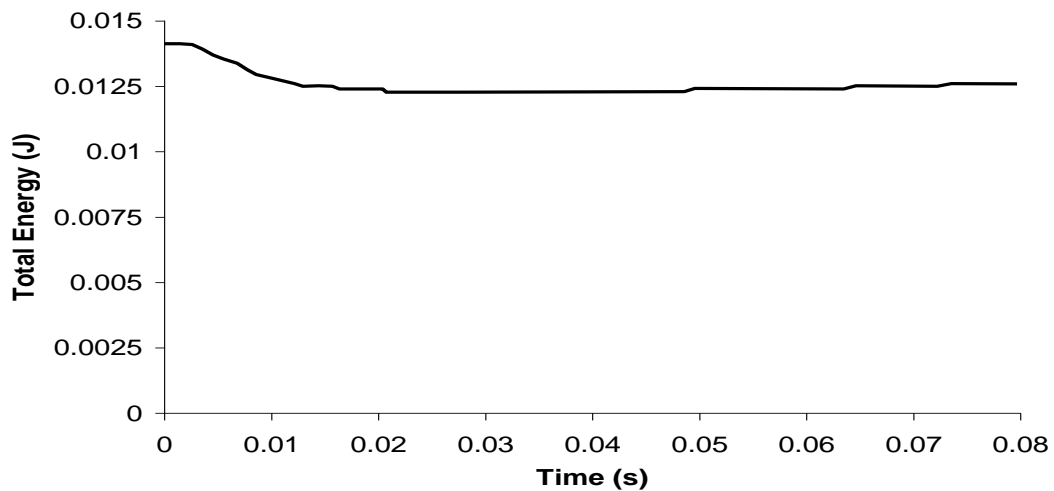


Fig. 6. Numerical model total energy, 1.64 kg impactor, 150 mm drop height, 20° deadrise angle.

A combined SPH / mesh-based modelling approach was taken, where an SPH region was defined in the immediate vicinity of the wedge, and a larger region of meshed Lagrangian elements used for the rest of the water tank. This approach was taken to balance the need for an SPH region to capture the high deformation around the impactor, with the computational efficiency of the Lagrangian elements. Detailed parametric investigations were conducted to verify the equivalence of SPH, Lagrangian and combined models, and to determine the most suitable dimensions of the SPH region to balance accuracy and computational efficiency. Further investigations were conducted on the particle density, summarised in Table 3, Fig. 4 and Fig. 5, where a small particle spacing (1 mm) was required to capture the detailed behaviour of the fluid flow.

Following the investigations on the combined SPH and Lagrangian regions, the particle density, and other preliminary investigations on the wedge depth, gravitational acceleration, symmetry, particle approximation theory and smoothing lengths, the baseline parameters for all models were defined and are summarised in Table 4.

All models were simulated using a single 2.3 GHz AMD Opteron processor with 4 GB DDR memory, with run times typically around 23 hours. The conservation of energy was reasonably good across all simulations. Fig. 6 shows the predicted total energy for the highest impact energy simulation, which corresponded to the largest energy variation. In this simulation, a variation in total energy of 13% was seen, and for other simulations the energy variation was on average around 10%.

4. RESULTS AND DISCUSSION

The results of the experimental and numerical investigations are summarised in Fig. 7 to Fig. 13, where Fig. 7 to Fig. 9 shows the maximum section force for each configuration, Fig. 10 to Fig. 12 are selected fluid flow sequences, and Fig. 13 shows the effect of increasing deadrise angle on the force-time history.

From the results in Fig. 7 to Fig. 9 and Fig. 13, increasing the deadrise angle decreased the maximum impact force and decreased the impact duration. These are well-known phenomena, caused by low angle wedges producing a more bluff or “slamming” water entry (Chuang 1966). Similarly, from the results in Fig. 7 to Fig. 9, increasing the drop height increased the maximum impact force, due to the increased impact energy.

The results for the 1.64 kg impactor show the most variation from these general trends, as seen in Fig. 7. For this impactor, increased maximum forces were not always seen for lower deadrise angles and increased drop heights, particularly at low deadrise angles and for the 150 mm drop height. It is unclear whether these tests involved more experimental error, particularly as the numerical analyses predicted the same trends.

The fluid flow images from the experiment in Fig. 2 and Fig. 10 to Fig. 12 show that a largely 2D flow field was generated. The rise up of the water along the wedge face was clearly captured and symmetric flow patterns

were observed along both sides of the wedge. Some water is evident in the 2 mm gap between the wedge face and the glass tank, though given the size of this relative to the depth of the wedge (333 mm), its effect is considered small.

The experimental results for section force were influenced by the error involved in the data acquisition process. The manual identification of points using the Tracker software was the source of some error in the experimental measurement, caused by the subjective nature of the measurement. The small size of the points was also problematic, as given the resolution of the camera each point had a diameter of around six pixels. The presence of water in the gap between the wedge face and glass tank also caused difficulties in point identification in some instances. The influence of these errors was investigated by taking six independent acquisitions from the same test data, and studying the variation between acquisitions. An example of this study for one configuration is shown in Fig. 14. It was found that the coefficient of variance (standard deviation / average) was typically around 10% for all configurations, though as high as 14% for tests involving the lowest acceleration values.

For the numerical analysis, close comparison with experimental results was seen across almost all configurations, particularly in consideration of the experimental variance with acquisition. The results in Fig. 7 to Fig. 9 show that the maximum section force was predicted well, with the trends were well captured, particularly for large deadrise angles. As the deadrise angle decreased and the degree of slamming impact increased, the numerical models predicted higher maximum wedge forces than seen in the experiments. The largest variation between experiment and numerical predictions was 65%, though in general the variation was within 15%, and mostly within 10% for deadrise angles 30° and greater.

The fluid flow patterns in Fig. 10 to Fig. 12 show excellent qualitative comparison between the experiment and numerical predictions, as a result of the high particle density. The closest correlation was seen with the 40° wedge impact in Fig. 12, where the rate of water rise along the wedge face, and the fluid pattern with the water passed the wedge chine showed excellent agreement. For the 20° wedge (Fig. 10), the numerical model predicted a faster water rise along the wedge and a greater volume of displaced water. These findings correlate with the general over-prediction of section forces for low angles, and the close comparison with experimental data seen for large deadrise angles. Application of a finer mesh density in the region immediately around the wedge face would be required to more accurately capture the behaviour of the low deadrise angle wedges.

Overall, the results in this investigation indicate that the combination of SPH and mesh-based regions allows for a suitable combination of accuracy and computational efficiency. This has application for more complex analysis, such as aircraft ditching investigations, where the size of the models required would be considerably larger. Further, the results in this work demonstrated an energy variation of around 10%. Preliminary studies into this energy variation revealed

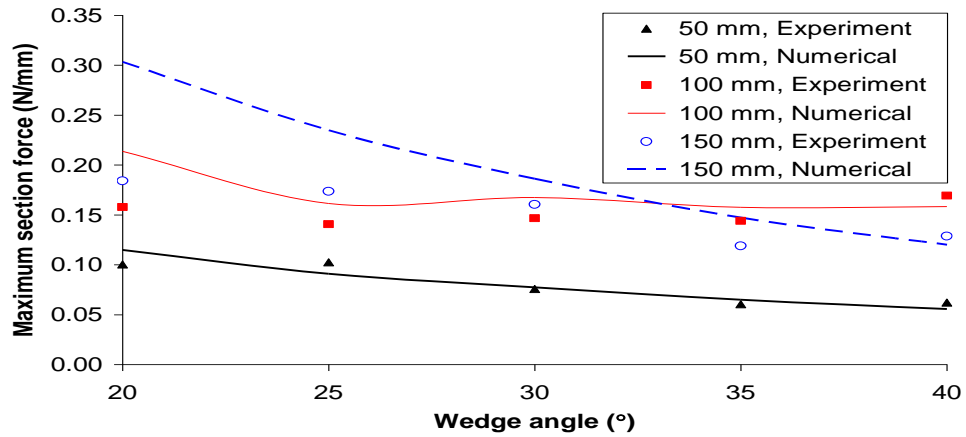


Fig. 7. Maximum section force, 1.64 kg impactor, varying drop height.

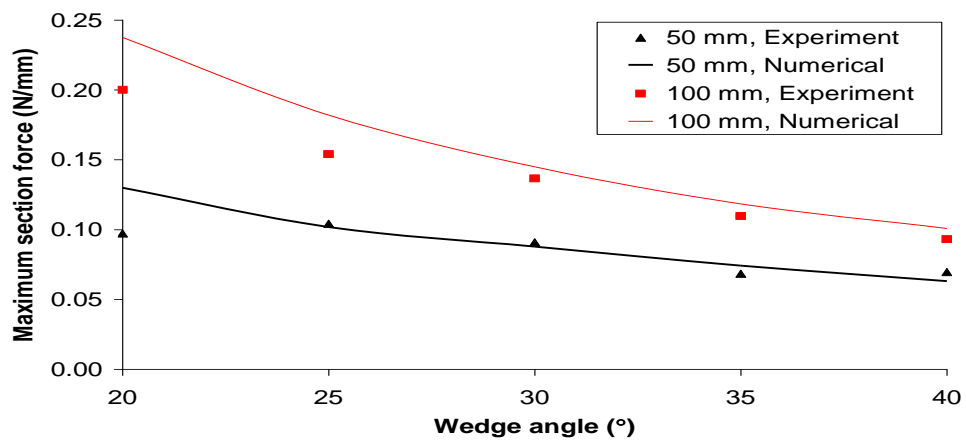


Fig. 8. Maximum section force, 1.85 kg impactor, varying drop height.

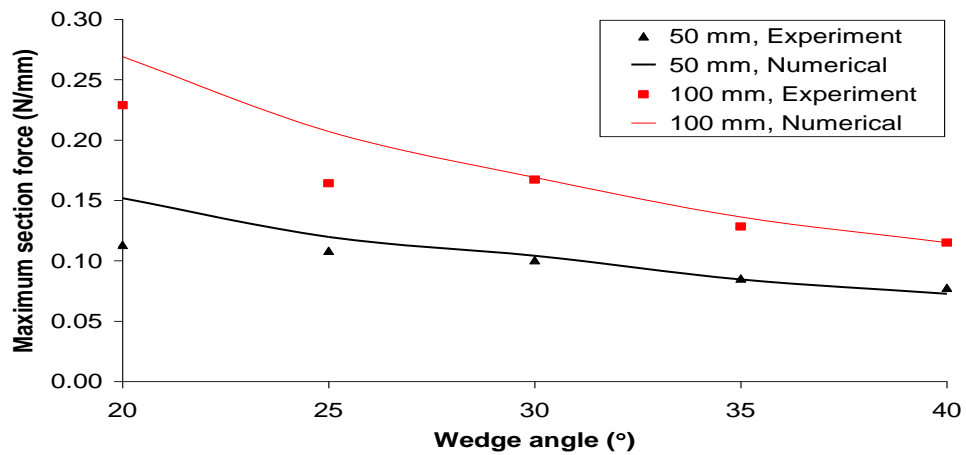


Fig. 9. Maximum section force, 2.07 kg impactor, varying drop height.

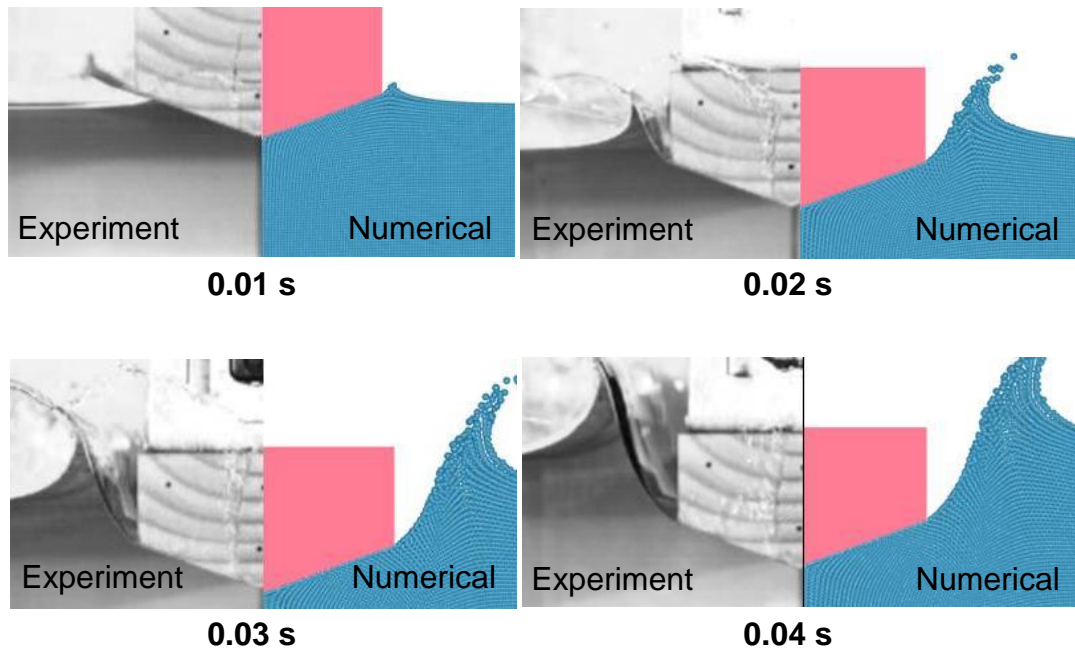


Fig. 10. Fluid flow, 1.64 kg impactor, 150 mm drop height, 20° deadrise angle

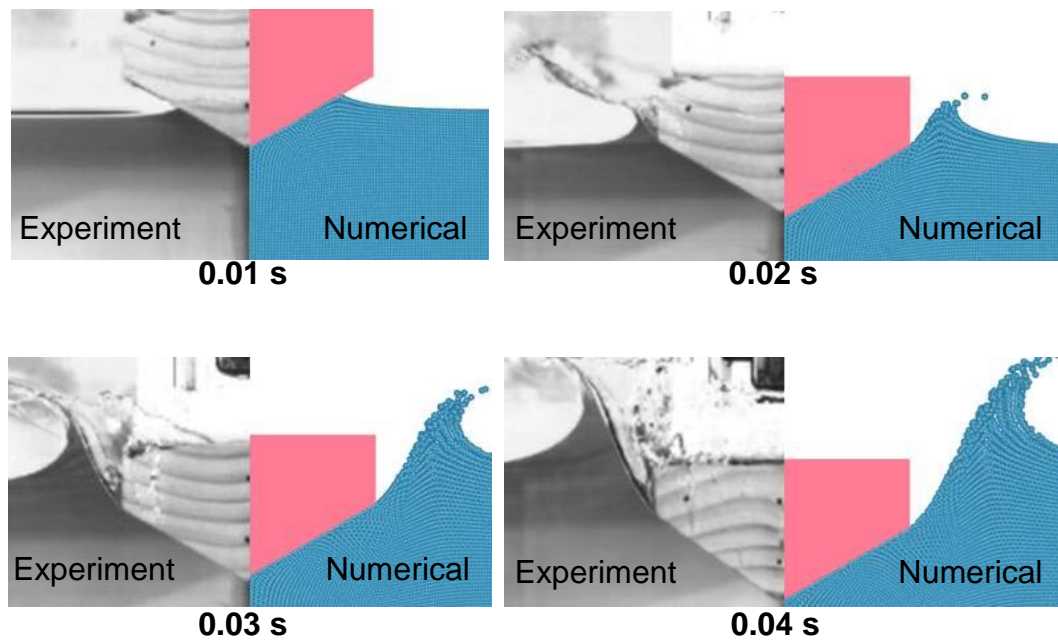


Fig. 11. Fluid flow, 1.64 kg impactor, 150 mm drop height, 30° deadrise angle.

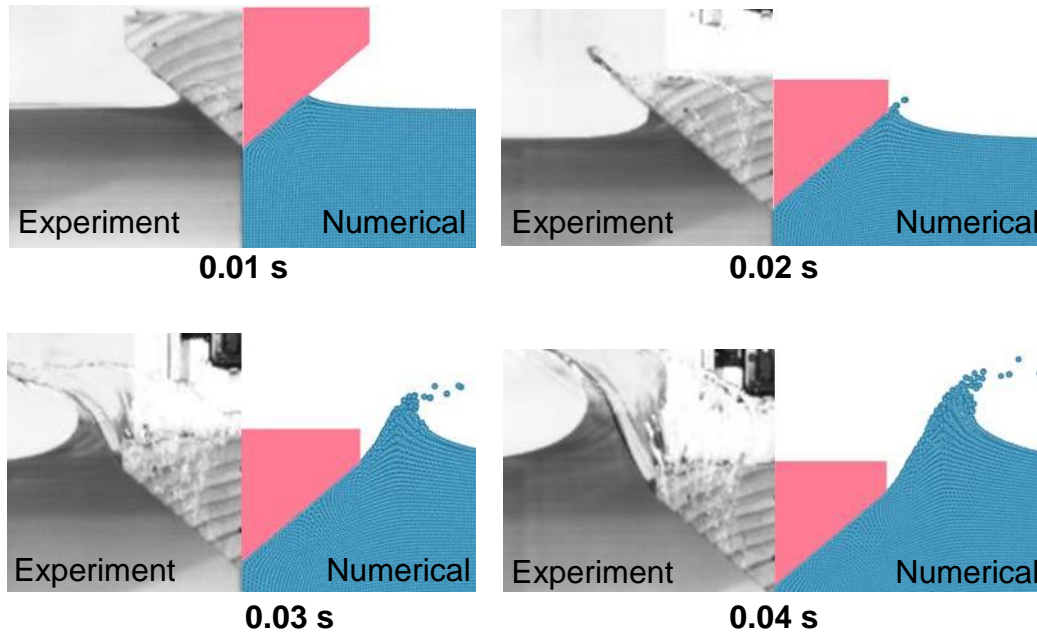


Fig. 12. Fluid flow, 1.64 kg impactor, 150 mm drop height, 40° deadrise angle.

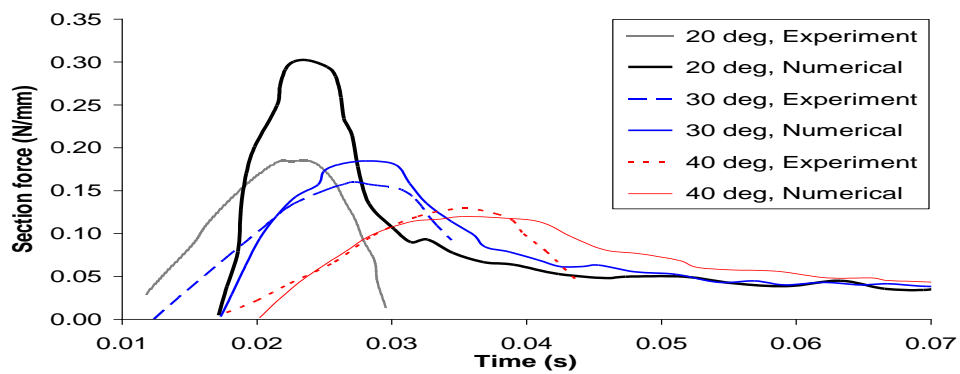


Fig. 13. Section force, 1.64 kg impactor, 150 mm drop height, varying deadrise angle.

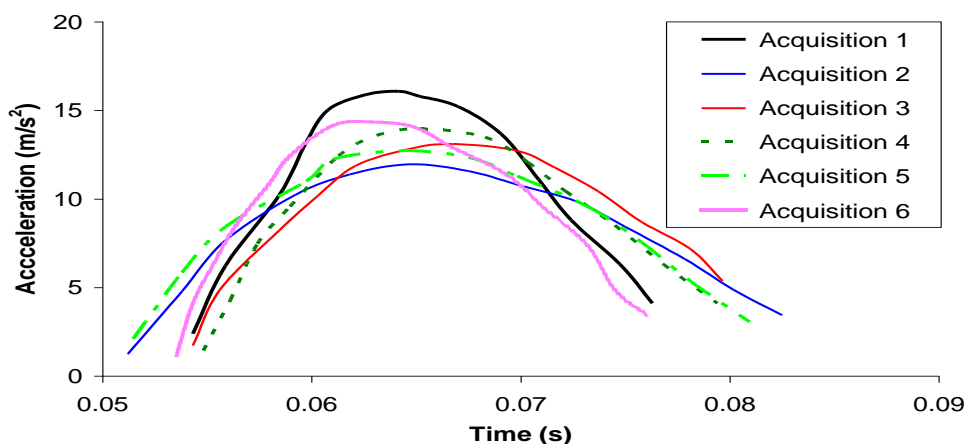


Fig. 14. Variation in experimental acceleration results for multiple acquisitions, 1.64 kg impactor, 50 mm drop height, 20° deadrise angle.

that larger variations were seen for larger SPH regions and coarser particle densities. In this respect, the technique applied in this work of combining a small SPH region of high particle density with a mesh-based

region is highly suited for larger models as a means of minimising the energy variation from the SPH analysis.

5. CONCLUSION

Drop test experiments were conducted involving symmetric rigid wedges of varying deadrise angle and mass impacted into water to generate a 2D flow field. The kinematic behaviour of the wedge and water was recorded and characterised using a high-speed video camera. Numerical models were analysed in LS-DYNA® that combined SPH and mesh-based regions. The numerical analysis was found to be capable of capturing the majority of experimental results and trends, within the bounds of the experimental variance. The modelling strategy of combining a high particle density SPH region with a Lagrangian mesh-based region was also found to be computationally efficient and to minimise the energy variation associated with the SPH analysis. Further, the experimental results for fluid flow patterns and wedge kinematics were demonstrated as a valuable database for assessment of numerical models.

ACKNOWLEDGEMENTS

The authors acknowledge RMIT technical officers for assistance with rig design and experimental testing, Mr Chetan Chandra or RMIT University for assistance with experiment and modelling, and the support provided by the Australian Government's International Postgraduate Research Scholarships (IPRS) scheme.

REFERENCES

- Anghileri, M., L.-M.L. Castelletti, E. Francesconi, A. Milanese, and M. Pittofrati. (2011). Rigid body water impact-experimental tests and numerical simulations using the SPH method. *Journal of Impact Engineering*. 38, 141-151.
- Anghileri, M., L.-M.L. Castelletti, E. Francesconi, A. Milanese, and M. Pittofrati. (2014). Survey of numerical approaches to analyse the behavior of a composite skin panel during a water impact. *Journal of Impact Engineering*. 63, 43-51.
- Brown, D. (2011). Tracker - Free video analysis and modelling tool for physics education, in: <www.cabrillo.edu/~dbrown/tracker> (accessed 29 September 2011).
- Campbell, J.C., and R. Vignjevic. (2012). Simulating structural response to water impact. *Journal of Impact Engineering*. 49, 1-10.
- Chuang, S.-L. (1966). *Slamming of rigid wedge-shaped bodies with various deadrise angles*. Washington, DC, USA: Department of the Navy.
- Fasanella, E.L., K.E. Jackson, C.E. Sparks, and A.K. Sareen. (2003, May). Water impact test and simulation of a composite energy absorbing fuselage section, in: *American Helicopter Society 59th Annual Forum*, Phoenix, Arizona, USA.
- Gingold, R.A., and J.J. Monaghan. (1977). Smoothed particle hydrodynamics - Theory and application to non-spherical stars, *Monthly Notices of the Royal Astronomical Society*. 181, 375-389.
- Groenenboom, P.H.L., and B.K. Cartwright. (2010). Hydrodynamics and fluid-structure interaction by coupled SPH-FE method. *Journal of Hydraulic Research*. 48(S1), 61-73.
- Hallquist, J.O. (2006). *LS-DYNA® Theory Manual*, Livermore, California, USA: Livermore Software Technology Corporation.
- Liu, G.R., and M.B. Liu. (2003). *Smoothed particle hydrodynamics - a meshfree particle method*. Singapore: World Scientific Publishing Co..
- Liu, M.B., and G.R. Liu. (2010). Smoothed particle hydrodynamics (SPH): An overview and recent developments. *Archives of Computational Methods in Engineering*. 17(1), 25-76.
- Oger, G., M. Doring, B. Alessandrini, and P. Ferrant. (2006). Two-dimensional SPH simulations of wedge water entries. *Journal of Computational Physics* 213, 803-822.
- Panciroli, R. (2013). Hydroelastic impacts of deformable wedges. In: Abrate, S., Castanié, B., and Rajapakse, Y.D.S. (eds). *Dynamic Failure of Composite and Sandwich Structures*. Dordrecht, The Netherlands: Springer.
- Pentecôte, N., and A. Vigliotti. (2003). Crashworthiness of helicopters on water: Test and simulation of a full-scale WG30 impacting on water. *International Journal of Crashworthiness* 8, 559-572.
- Pentecôte, N., D. Kohlgruber, and A. Kamoulakos. (2003, December). Simulation of water impact problems using the smoothed particle hydrodynamics method. In: *International Conference on Technological Innovation for Land Transportation (TILT)*, Lille, France.